Calculations of mesic (K^-, η) nuclei

J. Mares

Nuclear Physics Institute, Rez

+

A. Cieply, J. Hrtankova, M. Schäfer

(NPI, Rez)

B. Bazak, N. Barnea, E. Friedman, A. Gal

(the Hebrew University, Jerusalem)

3*rd* Jaggiellonian Symposium on Fundemantal and Applied Subatomic Physics,

Krakow, 24 - 28 June, 2019

$\bar{K}N$ *and* ηN *interactions*

- chiral $\mathrm{SU}(3)_L \times \mathrm{SU}(3)_R$ meson-baryon effective Lagrangian for $\{\pi, K, \eta\} + \{N, \Lambda, \Sigma, \Xi\}$
- $\exists$ resonances (e.g. $\Lambda(1405)$) $\Rightarrow$ χPT not applicable $\rightarrow$
- nonperturbative coupled-channel resummation techniques

$$T_{ij} = V_{ij} + V_{ik} G_{kl} T_{lj}, \quad V_{ij} \text{ derived from } \mathcal{L}_\chi$$

Effective potentials are constructed to match the chiral meson-baryon amlitudes (up to NLO order)

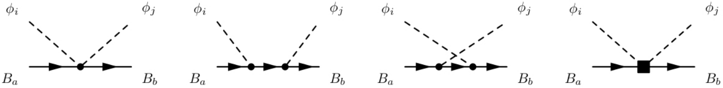

$\mathcal{O}(q^1)$ contact — direct s-term — crossed u-term — $\mathcal{O}(q^2)$ contact

$K^- N$ *and* ηN *interactions*

- Channels involved:
  $\pi\Lambda,\ \pi\Sigma,\ \bar{K}N,\ \eta\Lambda,\ \eta\Sigma,\ K\Xi \qquad (S=-1)$
  $\pi N,\ \eta N,\ K\Lambda,\ K\Sigma,\ (\eta' N) \qquad (S=0)$

- Model parameters fixed in fits to low-energy meson-nucleon data:

- $S=-1$ sector ($\bar{K}N$ related channels)
  - kaonic hydrogen data (SIDDHARTA)
  - $K^- p$ threshold branching ratios
  - $K^- p$ low energy X-sections

- $S=0$ sector (ηN related channels)
  - πN amplitudes from SAID database (S_{11} and S_{31} partial waves)
  - $\pi^- p \to \eta n$ reaction X-sections
  - P. C. Bruns, A. Cieply, arXiv:1903.10350 [nucl-th]
    η_0 meson singlet field included explicitly
    $\pi^- p \to K^0\Lambda$ and $\pi^- p \to \eta' n$ reaction X-sections

K^-N scattering amplitudes (free space)

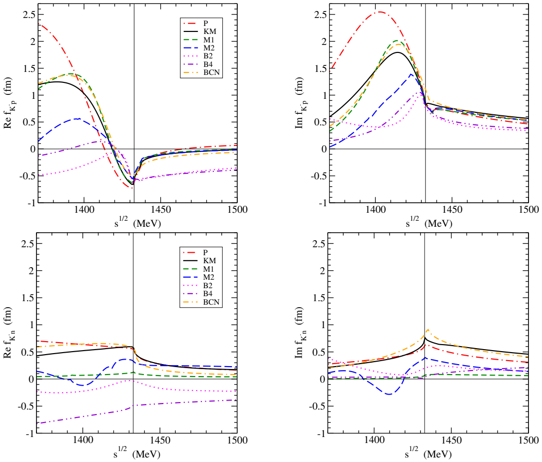

Prague (P)	A. Cieply, J. Smejkal, Nucl. Phys. A 881 (2012) 115
Kyoto-Munich (KM)	Y. Ikeda, T. Hyodo, W. Weise, Nucl. Phys. A 881 (2012) 98
Murcia (M1 and M2)	Z. H. Guo, J. A. Oller, Phys. Rev. C 87 (2013) 035202
Bonn (B2 and B4)	M. Mai, U.-G. Meiner, Nucl. Phys. A 900 (2013) 51
Barcelona (BCN)	A. Feijoo, V. Magas, A. Ramos, Phys. Rev. C99 (2019) 035211

ηN scattering amplitudes (free space)

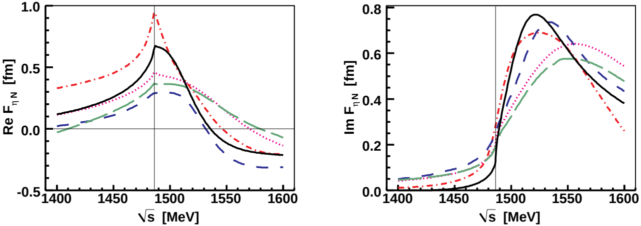

line	$a_{\eta N}$ [fm]	model
dotted	0.46+i0.24	N. Kaiser, P.B. Siegel, W. Weise, PLB 362 (1995) 23
short-dashed	0.26+i0.25	T. Inoue, E. Oset, NPA 710 (2002) 354 (GR)
dot-dashed	0.96+i0.26	A.M. Green, S. Wycech, PRC 71 (2005) 014001 (GW)
long-dashed	0.38+i0.20	M. Mai, P.C. Bruns, U.-G. Meißner, PRD 86 (2012) 094033 (M2)
full	0.67+i0.20	A. Cieply, J. Smejkal, Nucl. Phys. A 919 (2013) 334 (CS)

ηN scattering amplitudes (free space)

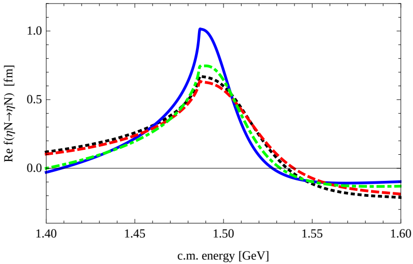

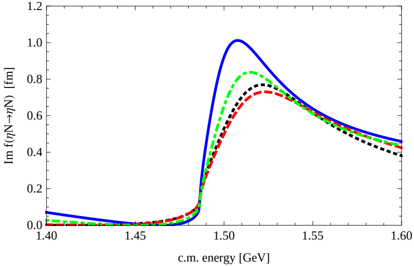

An explicit inclusion of the singlet meson field η_0 leads to a more attractive ηN interaction – compare the case with $\eta_0 - \eta_8$ mixing (blue line) and without $\eta_0 - \eta_8$ mixing (the CS model, black dotted line) - P. C. Bruns, A. Cieply, arXiv:1903.10350 [nucl-th]

$\bar{K}N$ *vs.* η *amplitudes*

- Strong energy dependence of the scattering amplitudes !

	$E_{\rm th}$ (MeV)	resonance
$\bar{K}N$	1434	$\Lambda(1405)$
ηN	1486	$N^*(1535)$

$\Lambda(1405)$ resonance below threshold

vs.

$N^*(1535)$ resonance above threshold

Energy dependence

- K^-N amplitudes are a function of $\sqrt{s}$
  $(s = (E_N + E_{K^-})^2 - (\vec{p}_N + \vec{p}_{K^-})^2)$

- K^-N cms frame $\rightarrow$ K^--nucleus frame $\vec{p}_N + \vec{p}_{K^-} \neq 0$
  A. Cieplý, E. Friedman, A. Gal, D. Gazda, J. Mareš, Phys. Lett. B 702 (2011) 402
  e.g., in many body systems (atoms, nuclei):

$$\sqrt{s} = E_{th} - B_N \frac{\rho}{\bar{\rho}} - \xi_N \left[B_{K^-} \frac{\rho}{\rho_{max}} + 23 \left(\frac{\rho}{\bar{\rho}}\right)^{2/3} + V_C \left(\frac{\rho}{\rho_{max}}\right)^{1/3} \right] + \xi_{K^-} \mathrm{Re} V_{K^-}(r) \ ,$$

  where $B_N = 8.5$ MeV and $\xi_{N(K^-)} = m_{N(K^-)}/(m_N + m_{K^-})$;
  Low-density limit $\delta\sqrt{s} \rightarrow 0$ as $\rho \rightarrow 0$, where $\delta\sqrt{s} = \sqrt{s} - E_{th}$.

- B_{K^-} and V_{K^-} $\Rightarrow$ self-consistency scheme

- For few - body η nuclear systems:
  $\langle \delta\sqrt{s} \rangle = -\frac{B}{A} - \frac{A-1}{A} B_\eta - \xi_N \frac{1}{A} \langle T_N \rangle - \xi_A \xi_\eta \left(\frac{A-1}{A}\right)^2 \langle T_\eta \rangle$,
  where $\Xi_A = (A m_N/(A m_N + m_\eta)$, T_N (T_η) is nuclear (η) kinetic energy

Energy shift in η nuclei

- In-medium (subthreshold) energy shift:

$$\delta\sqrt{s} = -B_N \frac{\rho}{\bar{\rho}} - \xi_N B_\eta \frac{\rho}{\rho_0} - \xi_N T_N (\frac{\rho}{\rho_0})^{2/3} + \xi_\eta \mathrm{Re} V_\eta(\sqrt{s}, \rho)$$

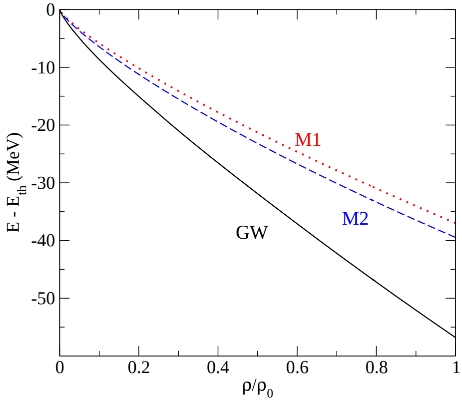

- B_η, V_η, ρ $\Rightarrow$ selfconsistent solution $\rightarrow$

  40 - 60 MeV energy shift at ρ_0 – larger than shift by B_η (GR) or by 30 MeV (Haider, Liu)

Sensitivity to the energy shift

- selfconsistent $\delta\sqrt{s}$ reduces both 1s B_η and Γ_η

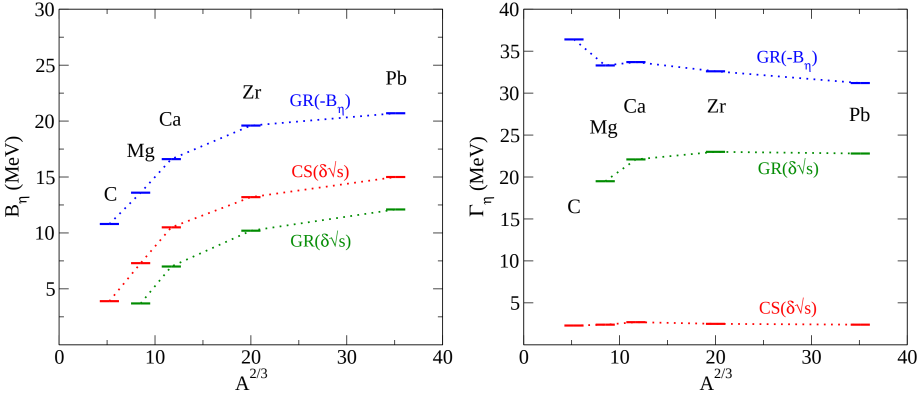

In-medium K^-N (ηN) amplitudes

nuclear medium impact: Pauli (anti)correlations, hadron self-energies

- WRW method (based on multiple scattering theory)
  T. Wass, M. Rho, W. Weise, Nucl. Phys. A 617 (1997) 449

$$F_1 = \frac{\frac{\sqrt{s}}{m_N} F_{K^-n}(\sqrt{s})}{1 + \frac{1}{4}\xi_k \frac{\sqrt{s}}{m_N} F_{K^-n}(\sqrt{s})\rho}\,, \quad F_0 = \frac{\frac{\sqrt{s}}{m_N}[2F_{K^-p}(\sqrt{s}) - F_{K^-n}(\sqrt{s})]}{1 + \frac{1}{4}\xi_k \frac{\sqrt{s}}{m_N}[2F_{K^-p}(\sqrt{s}) - F_{K^-n}(\sqrt{s})]\rho}$$

$$\text{where} \quad \xi_k = \frac{9\pi}{p_F^2} 4\int_0^\infty \frac{dt}{t} \exp(iqt)\, j_1^2(t), \quad q = \frac{1}{p_F}\sqrt{{\omega_{K^-}}^2 - m_{K^-}^2}\,.$$

- P + Pauli + SE model (Green function integral modified)
  A. C., E. Friedman, A. Gal, D. Gazda, J. Mareš, Phys. Rev. C 84 (2011) 045206

$$F_{ij}(\sqrt{s};\rho) = \left[V^{-1}(\sqrt{s}) - G(\sqrt{s};\rho)\right]^{-1}_{ij}$$

$$G_j(\sqrt{s};\rho) = -4\pi \int_{\Omega_j(\rho)} \frac{d^3p}{(2\pi)^3} \frac{g_j^2(p)}{p_j^2 - p^2 - \Pi_j(\sqrt{s},\vec{p};\rho) + \mathrm{i}0}$$

In-medium modified $\bar{K}N$ amplitudes

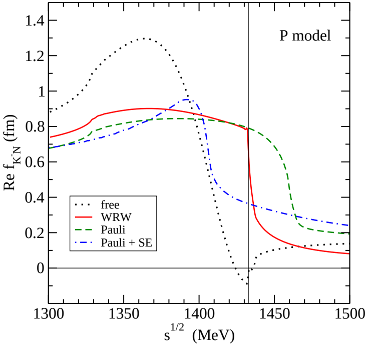

Energy dependence of reduced free-space (dotted line) $f_{K^-N} = \frac{1}{2}(f_{K^-p} + f_{K^-n})$ amplitude compared with WRW modified amplitude (solid line), Pauli (dashed line), and Pauli + SE (dot-dashed line) modified amplitude for $\rho_0 = 0.17$ fm^{-3} in the P model.

η in few-body systems

Variational calculations (hypersherical basis , Stochastic Variational Method (SVM))

N. Barnea, E. Friedman, A. Gal, PLB 747 (2015) 345, NPA 968 (2017) 35;

M.Schäfer, N. Barnea, E. Friedman, A. Gal, J. Mares, EPJ Web Conf. 199, 02022 (2019)

- NN: Argonne AV4', Minnesota MN potential
- ηN: complex E-dep. local potential derived from the chiral coupled-channels model:

  $$v_{\eta N}(E,r) = -\frac{4\pi}{2\mu_{\eta N}} b(E)\rho_\Lambda(r),$$

  where $E = \sqrt{s} - \sqrt{s_{\rm th}}$, $\quad \rho_\Lambda(r) = (\frac{\Lambda}{2\sqrt{\pi}})^3 exp\left(-\frac{\Lambda^2 r^2}{4}\right)$

  $b(E)$ fitted to phase shifts δ derived from $F_{\eta N}(E)$ in GW and CS models;

  scale Λ inversely proportional to the $v_{\eta N}$ range

- π-less EFT at LO - N. Barnea, B. Bazak, E. Friedman, A. Gal, PLB 771 (2017) 297

ηNN, η^3He, η^4He *and* η^6Li *systems*

ηNN

- unbound

(N. Barnea, E. Friedman, A. Gal, Phys. Lett. B 747 (2015) 345)

$\eta^3 He$

$V_{\eta N}$	V_{NN}	$\delta\sqrt{s_{sc}}$	B_η	Γ_η
GW, $\Lambda = 2$	MN	-9.385	0.099	1.144
	AV4'	-11.478	-0.028	0.769
GW, $\Lambda = 4$	MN	-13.392	0.990	3.252
	AV4'	-14.881	0.686	2.438
CS, $\Lambda = 2$	MN	-8.388	-0.217	0.057
CS, $\Lambda = 4$	MN	-8.712	-0.161	0.227

(N. Barnea, E. Friedman, A. Gal, Nucl. Phys. A 968 (2017) 35)

MN - (D. R. Thomson, M. LeMere, Y. C. Tang, Nucl. Phys. A 286 (1977) 53)

AV4' - (R. B. Wiringa, S. C. Pieper, Phys. Rev. Lett. 89 (2002) 182501)

ηNN, η^3He, η^4He *and* η^6Li *systems*

		$\eta^4 He$ [1]			$\eta^6 Li$ [2]		
$V_{\eta N}$	V_{NN}	$\delta\sqrt{s_{sc}}$	B_η	Γ_η	$\delta\sqrt{s_{sc}}$	B_η	Γ_η
GW, $\Lambda = 2$	MN	-19.48	0.96	1.98	-21.47	2.17	3.00
	AV4'	-23.65	0.38	1.21	-	-	-
GW, $\Lambda = 4$	MN	-29.75	4.69	4.50	-33.11	6.40	4.90
	AV4'	-32.41	3.51	3.62	-	-	-
CS, $\Lambda = 2$	MN	-16.70	-0.16	0.13	-16.07	-0.08	0.85
CS, $\Lambda = 4$	MN	-19.25	0.47	0.90	-21.08	0.68	1.44

1 (N. Barnea, E. Friedman, A. Gal, Nucl. Phys. A 968 (2017) 35)

2 (M.Schäfer, N. Barnea, E. Friedman, A. Gal, J. Mares, EPJ Web Conf. 199, 02022 (2019), η^6Li calculated only for MN V_{NN} potential

Imaginary part of the $V_{\eta N}$ potential

$\Gamma_\eta = -2\langle\Psi_{\rm gs}|{\rm ImV}_{\eta{\rm N}}|\Psi_{\rm gs}\rangle$ (real) vs. solution of eigenvalue problem for a complex Hamiltonian (imaginary part of the $V_{\eta N}$ included) (cmplx)

η^3He *and* η^4He *systems (for MN and GW potentials)*

η^3He		B_η [MeV]	Γ_η [MeV]	$\delta\sqrt{s_{sc}}$ [MeV]
$\Lambda = 2$	(real)	0.11	1.37	-9.23
	(cmplx)	-0.25	1.32	-8.87
$\Lambda = 4$	(real)	1.01	3.32	-13.18
	(cmplx)	0.36	3.44	-12.72

η^4He		B_η [MeV]	Γ_η [MeV]	$\delta\sqrt{s_{sc}}$ [MeV]
$\Lambda = 2$	(real)	0.97	2.17	-19.64
	(cmplx)	0.77	2.22	-19.50
$\Lambda = 4$	(real)	4.62	4.38	-29.73
	(cmplx)	4.40	4.41	-29.60

Coulomb interaction included

- ${\rm Im}\,V_{\eta N}$ acts as a repulsion decreasing the binding of η
- effect of ${\rm Im}\,V_{\eta N}$ is rather significant in η^3He (close to the threshold), decreases in η^4He (larger $\delta\sqrt{s_{sc}}$), and becomes negligible in η^6Li

K^- (η) *in nuclear matter*

chirally motivated K^-N (ηN) amplitudes in a free space

$\Downarrow$

in-medium amplitudes

$\Downarrow$

K^- (η)-nuclear optical potential

$\Downarrow$

solve the Klein-Gordon equation to get K^- (η)-nuclear (or K^--atomic) states

- accounting for Pauli principle (and hadron self-energies)
- energy dependence of the optical potential treated self-consistently

Kaonic atoms analysis

E. Friedman, A. Gal, Nucl. Phys. A 959 (2017) 66 :

- χ^2 fits to kaonic atoms data (energy shifts, widths and yields = upper level widths)
- optical potentials $V_{K^-} = V_{K^-}^{(1)}$ constructed from the chirally motivated amplitudes fail to describe the data
- K^- interactions with two and more nucleons are needed, e.g. $K^- + N + N \to Y + N$

  $$2\mathrm{Re}(\omega_{K^-})\, V_{K^-}^{(2)} = -4\pi\, B\, (\frac{\rho}{\rho_0})^\alpha \rho$$

  where B is a complex parameter and α is positive
- total K^- optical potential $V_{K^-} = V_{K^-}^{(1)} + V_{K^-}^{(2)}$
  such a potential derived for each chiral model fits the K^- atom data

Kaonic atoms analysis

additional constraint - fractions of single-/multi- nucleon absorption at rest:

H. Davis et al., Nuovo Cimento 53 (1968) 313 (Berkeley);
J.W. Moulder et al., Nucl. Phys. B35 (1971) 332 (BNL);
C. Vander Velde-Wilquet et al., Nuovo Cimento 39A (1977) 538 (CERN)

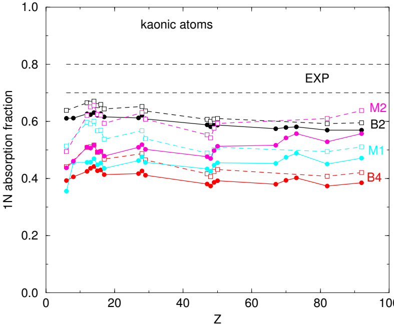

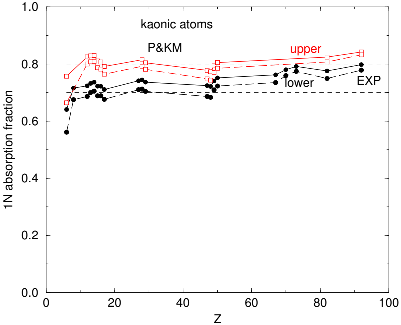

Fraction of single-nucleon absorption for the chiral approaches. Solid circles for lower states, open squares for upper states. Left: B2, B4, M1 and M2, Right: P1, KM1 for $\alpha = 1$ (solid) and P2, KM2 for $\alpha = 2$ (dashed).

Only P, KM and BCN models found acceptable.

K^- optical potential

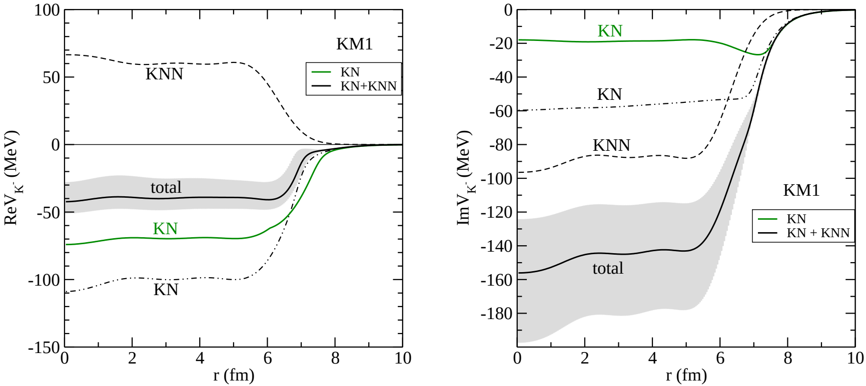

The respective contributions from K^-N and K^-NN potentials to the total real and imaginary K^- optical potential in the ^{208}Pb$+K^-$ nucleus, calculated self-consistently in the KM1 model (the FD variant). The single-nucleon K^- potential (green solid line) of the KM model is shown for comparison. Shaded area = uncertainties in the KNN part input.

J. Hrtankova, J. Mares, Phys. Lett. B 770 (2017) 342; Phys. Rev. C 96, 015205 (2017)

K^-N vs. K^-NN absorption in ^{208}Pb

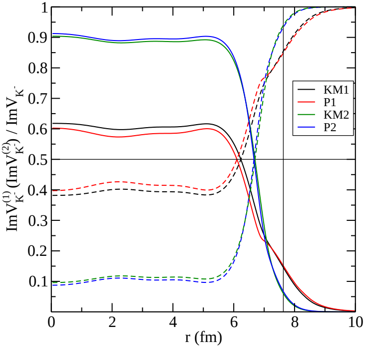

Ratios of $\mathrm{Im}\,V^{(1)}_{K^-}$ and $\mathrm{Im}\,V^{(2)}_{K^-}$ potentials to the total $\mathrm{Im}\,V_{K^-}$ as a function of radius, calculated self-consistently for the $^{208}\mathrm{Pb}+K^-$ system using the KM and P models. The vertical lines mark the *nuclear surface density* of $0.15\,\rho_0$.

$\bar{K}NN$ absorption dominates in nuclear interior, the $\bar{K}N$ absorption at low densities.

K^- 1s binding energies and widths

... when the K^-NN phenomenological term $V^{(2)}_{K^-} \sim B\,(\rho/\rho_0)^\alpha$ ($\alpha = 1$ or 2) is added, some states are not bound and the absorption widths become larger than the corresponding binding energies

KM model			$\alpha = 1$		$\alpha = 2$	
		KN	HD	FD	HD	FD
^{16}O	B_{K^-}	45	34	not	48	not
	Γ_{K^-}	40	109	bound	121	bound
^{40}Ca	B_{K^-}	59	50	not	64	not
	Γ_{K^-}	37	113	bound	126	bound
^{208}Pb	B_{K^-}	78	64	33	80	53
	Γ_{K^-}	38	108	273	122	429
P model			$\alpha = 1$		$\alpha = 2$	
^{16}O	B_{K^-}	64	49	not	63	not
	Γ_{K^-}	25	94	bound	117	bound
^{40}Ca	B_{K^-}	81	67	not	82	not
	Γ_{K^-}	14	95	bound	120	bound
^{208}Pb	B_{K^-}	99	82	36	96	47
	Γ_{K^-}	14	92	302	117	412

J. Hrtankova, J. Mares, Phys. Lett. B 770 (2017) 342; Phys. Rev. C 96, 015205 (2017)

Microscopic model for in-medium $K^- NN$ absorption

Can we improve on the $K^- NN$ absorption? Earlier microscopic treatment in
T. Sekihara et al. - PRC 86, 065205 (2012) for the $K^- NN$, free space $\bar{K}N$ amplitudes
H. Nagahiro et al. - PLB 709, 87 (2012) for the $\eta' NN$ system
New work on the $\bar{K}NN$ system employs the in-medium BCN and P amplitudes:
J. Hrtankova, A. Ramos - prepared for publication (2019)

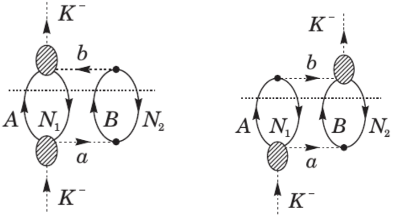

- $K^- NN$ self-energy

$$\Pi_{AB}(\vec{q}, q_0) = -\mathrm{i} t_{K^- N_1 \to Aa} t^*_{K^- N_1 \to Ab} V_{aBN_2} V_{bBN_2} \cdot \cdot \int \frac{d^4 q}{(2\pi)^4} U_{AN_1}(p-q) U_{BN_2}(q) q^2 \frac{1}{q^2 - m_a^2} \frac{1}{q^2 - m_b^2}$$

- t-matrices taken from chiral meson-baryon models

$K^- NN$ absorption

- AMADEUS measurement of the Λp to $\Sigma^0 p$ production rate in $K^- NN$ QF absorption

$$\mathcal{R} = \frac{\mathrm{BR}(K^- pp \to \Lambda p)}{\mathrm{BR}(K^- pp \to \Sigma^0 p)} = 0.7 \pm 0.2(stat.)^{+0.2}_{-0.3}(syst.)$$

R. Del Grande et al. - Eur. Phys. J. C79 (2019) 190

- two settings of the $K^- NN$ model used assuming $B_{K^-} = 0$ and 50 MeV;
  the Pauli blocked (WRW) amplitudes give the ratio $\mathcal{R}$ much closer to the experimental rate than the free amplitudes $\Rightarrow$ medium effects are relevant!

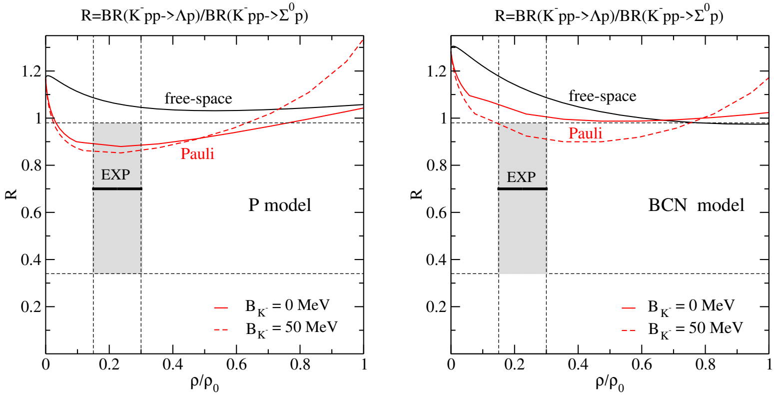

K^-NN absorption

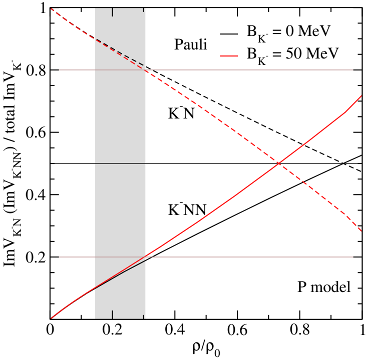

Ratio of single nucleon (K^-N) and two-nucleon (K^-NN) absoptive potentials to the total absorptive potential ($\mathrm{Im}\, V_{K-}$). The grey area shows the region of densities probed by low energy K^-.

$B_K = 0$ MeV - $\bar{K}NN$ starts to dominate at $\rho \sim \rho_0$
$B_K = 50$ MeV - $\bar{K}NN$ starts to dominate at $\rho \sim 0.7\, \rho_0$

Summary

- Chirally motivated models provide different predictions for the K^-N and ηN amplitudes at subthreshold energies.
- In-medium kaons (eta's) probe energies 50-100 MeV (40-60 MeV) below threshold. A realistic treatment of the energy dependence and in-medium modifications (Pauli blocking) is essential.
- Large energy shift and rapid decrease of the ηN amplitudes below threshold $\Rightarrow$ relatively small binding energies and widths of the calculated η nuclear states.
  Additional contribution to the η width due to $\eta N \rightarrow \pi\pi N$ and $\eta NN \rightarrow NN$ (not considered here) – estimated to add few MeV.
- ηd unbound, ${}^{3}_{\eta}$He unbound ?, ${}^{4}_{\eta}$He bound for the GW model
- Fits to kaonic atoms demonstrate the need of NN (or multinucleon) contribution to the K^--nuclear optical potential. The P, KM and BCN models satisfy the additional constraint of 1N to 2N absorption rate.
- The inclusion of multinucleon absorption in the calculations of K^- quasi-bound states in many-body systems leads to huge widths, considerably exceeding the binding energies. (The conclusion does not apply to few body K^--nucleons systems.)
- Microscopical model for K^-NN absorption in nuclear matter has been developed using chiral $\bar{K}N$ amplitudes. The preliminary results look encouraging, the ratio of Λp to $\Sigma^0 p$ production measured by AMADEUS is reproduced by the model when the in-medium amplitudes are employed.